



NLR TP 96344

## **A symmetrical boundary element formulation for sound transmission through cabin walls**

H. Schippers and F.P. Grooteman



## Summary

A symmetrical boundary element formulation is described for the transmission of sound through the panels of a cabin wall of an aircraft. The geometrical model consists of a double panel configuration including a cavity partly filled with porous material and with air. The acoustic pressure in the vibrating medium (air and porous material) is modelled by a boundary integral ansatz. The vibrating panels and the vibrating medium are coupled by the boundary condition for flexible walls. Classical boundary integral formulations result in a non-symmetric boundary element matrix, while the discretization of the Helmholtz equation using finite elements would yield a symmetrical stiffness matrix. In the present paper a symmetrical boundary element matrix is derived for the acoustic pressure inside and outside the cabin wall. The boundary elements are put on the panels of the cabin wall and on the interface between the air and the porous material. The computational costs of the present symmetrical boundary element formulation are comparable with the costs of classical boundary element formulations in acoustics, which are based on the direct method.

## Contents

<b>1</b>	<b>Introduction</b>	5
<b>2</b>	<b>Mathematical formulation</b>	7
<b>3</b>	<b>Boundary integral formulas for the acoustic pressure</b>	10
3.1	Boundary integral formula for the half-space $\Omega_i$	10
3.2	Boundary integral formula for a closed domain $\Omega$	11
<b>4</b>	<b>Boundary element discretization</b>	13
<b>5</b>	<b>Numerical implementation</b>	14
<b>6</b>	<b>Numerical results</b>	17
<b>7</b>	<b>Conclusions</b>	19
<b>8</b>	<b>References</b>	20

## 1 Introduction

Investigations on the acoustic field around and inside commercial aircraft are motivated by the urge to reduce cabin noise inside the aircraft. The exterior acoustic field causes vibrations of the cabin wall, which contribute to the interior noise. The cabin noise inside the aircraft can be reduced by putting porous acoustically absorbing material (insulation) just on the inside of the skin panel of the cabin wall.

In this paper a symmetrical boundary element is described for the transmission of sound through the panels of a cabin wall. The geometrical model consists of a double panel configuration including a cavity partly filled with porous material and with air (an illustration is given in figure 1). The lower panel is a stiffened skin panel, while the upper panel is an un-stiffened trim panel. The trim panel is backed by a semi-infinite room modelling the interior of the aircraft. The displacement of the skin panel is assumed to be given by the exterior acoustic field at the outer side of the aircraft. The sound transmission problem requires the calculation of the acoustic pressure in the air and in the porous material as well as the fluid-structure interaction with the un-stiffened trim panel. The acoustic pressure in the air and porous material is modelled by the Helmholtz equation (in the case of glass wool insulation with a complex wavenumber, which models the damping). The porous material is essentially assumed to be described by its porosity, resistivity, effective density and effective speed of sound, all of which are frequency dependent.

The acoustic pressure in the vibrating medium (air and porous material) is modelled by a boundary integral ansatz. The vibrating panels and the vibrating medium are coupled by the boundary condition for flexible walls. Classical boundary integral formulations result in a non-symmetric boundary element matrix, while the discretization of the Helmholtz equation using finite elements would yield a symmetrical stiffness matrix. In the present paper a symmetrical boundary integral formulation is described for the acoustic pressure inside and outside the cabin wall. The formulation maps the normal derivative of the pressure along the boundary on the pressure itself. In the case of a bounded domain (e.g. the volume covered by the porous medium or the volume covered by the air inside the cabin wall) the symmetrical boundary integral formulation has been taken from ref. 1. The symmetrical boundary element matrix follows from applying Galerkin's method. The present formulation is advantageous from the point of view that the boundary element matrix has the same mapping properties as the finite element matrix of the weak formulation of the Helmholtz equation. These properties are not preserved by the classical boundary element formulation, which yields an asymmetric system matrix. The basis and test functions are given by the classical piecewise linear functions on flat non-overlapping triangular elements.

The boundary elements are put on the panels of the cabin wall and on the interface between the air and the porous material. The computations involve the discretization of a hyper-singular integral operator, a weakly singular integral operator and a regular operator. The hyper-singular integral operator is regularized by integration of parts. Once this operator has been regularized, the computation of the coefficients of the corresponding boundary element matrix requires the same number of kernel evaluations as the computation of the coefficients of the weakly singular operator. Therefore, the computational costs of the present symmetrical boundary element formulation are comparable with the costs of classical boundary element formulations in acoustics, which are based on the direct method.

## 2 Mathematical formulation

In this section a mathematical model is presented for the transmission of sound through panels of a cabin wall. The model is applied to a double wall configuration of a cabin wall panel as shown in figure 1. It contains a closed cavity, partly filled with air and partly with porous material (e.g. glass wool). This cavity is given by the rectangular box  $\Omega_1$  in  $\mathbb{R}^3$ , with  $\Omega_1 = \Omega_{1,a} \cup \Omega_{1,g}$ . The boundary of  $\overline{\Omega_1}$  is denoted by  $\Gamma = \partial\overline{\Omega_1}$ . The unit normal vector  $n$  on  $\Gamma$  is pointing outwards, i.e. into  $\mathbb{R}^3 \setminus \overline{\Omega_1}$ . The boundary is split into three parts

$$\Gamma = \Gamma_1 \cup \Gamma_2 \cup \Gamma_3,$$

where  $\Gamma_1$  corresponds to the stiffened skin panel and  $\Gamma_3$  corresponds to the un-stiffened trim panel. The double wall configuration is assumed to be baffled in an infinite plate in the plane  $z = 0$ . The part of this plane that is not occupied by  $\Gamma_3$  is denoted by  $\Gamma_\infty$ .

Let the semi-infinite space given by  $z > 0$  be denoted by  $\Omega_i$  and the space denoted by the complement of  $\Omega_i \cup \overline{\Omega_1}$  in  $\mathbb{R}^3$  by  $\Omega_e$ . Here,  $\Omega_i$  and  $\Omega_e$  represent the interior and the exterior space of the aircraft cabin.

The transmission problem requires the modelling of the sound pressure in and outside the cabin wall as well as the fluid-structure interaction with the stiffened and un-stiffened panel. The problem is assumed to be time harmonic with angular frequency  $\omega$ . In the present paper the sound pressure in  $\Omega_e$  is not modelled. It is assumed that the acoustic field in  $\Omega_e$  as well as the induced displacement on  $\Gamma_1$  are known.

The acoustic pressure  $p$  in the regions  $\Omega_i$  and  $\Omega_{1,a}$  has to satisfy the Helmholtz equation

$$\Delta p + k^2 p = 0, \quad k = \frac{\omega}{c}, \quad (1)$$

where  $c$  is the speed of sound in air and  $k$  is the acoustic wave number. The acoustic pressure  $p$  in the region  $\Omega_{1,g}$  also has to satisfy the Helmholtz equation, but with a complex wave number  $\gamma$ ,

$$\Delta p + \gamma^2 p = 0, \quad (2)$$

where the definition of  $\gamma$  depends on the material properties of the porous medium. The porous material is essentially assumed to be described by its porosity  $h$ , resistivity  $\sigma$ , effective density

$\rho_e$  and effective speed of sound  $c_e$ , all of which are frequency dependent. For wave propagation in limp material (an approximate model for glass wool) the following expression for  $\gamma$  has been derived in Ref. 2

$$\gamma = (\omega/c_e)\sqrt{h\kappa(\omega)/\rho_e}, \quad \kappa(\omega) = \rho_e - (i\sigma/\omega)/(1 - \frac{i h \sigma}{\omega M}), \quad (3)$$

where  $M$  is the density of the fibre part. In the limp model the stiffness of the fibres is neglected. The limitation of the model is that the resonances in the porous material can not be described. This would require both stiffness and mass effects to be taken into account. As a consequence, the high frequency range (small wavelength) can not be calculated with sufficient accuracy. When the minimum acoustic wavelength of the computational problem is larger than the thickness of the porous layer, the assumption of the limp material holds.

The appropriate boundary conditions for  $p$  are

$$\frac{\partial p}{\partial n}(r) = \kappa(\omega)\omega^2 W(r), \quad r \in \Gamma_1 \quad (4)$$

$$= 0, \quad r \in \Gamma_2 \cup \Gamma_\infty \quad (5)$$

$$= \rho_a \omega^2 w(r), \quad r \in \Gamma_3. \quad (6)$$

At boundary  $\Gamma_1$  the normal displacement  $W$  of the skin panel is prescribed. The boundaries  $\Gamma_2$  and  $\Gamma_\infty$  are assumed to be acoustically hard. At boundary  $\Gamma_3$  the normal displacement  $w$  follows from solving an appropriate elastomechanical model for the trim panel. For reasons of explanation it is assumed in this section that the trim panel is isotropic and that the displacements are small, so that  $w$  is governed by the equations for a harmonically vibrating plate

$$\mathcal{L}(w) \equiv D\Delta^2 w - \omega^2 \delta \rho_s w = \mu, \quad (7)$$

where  $\Delta$  denotes the Laplace operator,  $D$  the bending stiffness of the plate,  $\rho_s$  its density and  $\delta$  its thickness. The right-hand side of (7) represents the load acting on the plate caused by the jump  $\mu$  in the acoustic pressure,

$$\mu = p^+ - p^-, \quad (8)$$

where  $p^+$  ( $p^-$ ) denotes the pressure on the upper (lower) side of the trim panel. In numerical investigations the elastomechanical operator  $\mathcal{L}$  will be modeled by four-noded finite shell elements. Note that the equations (1), (6), (7) and (8) define a coupled fluid-structure interaction problem.

At the fluid surface  $S$  between the porous material and the air two boundary conditions have to be satisfied. First, the pressure has to be continuous

$$p_g = p_a \tag{9}$$

and second the mass flow has to be continuous across the interface  $S$ . For glass-wool, having a porosity which is almost equal to unity, the mass flow continuity reduces to continuity of the normal displacement,

$$u_g^n = u_a^n = u_S^n. \tag{10}$$

Far away from the double wall configuration it is required that  $p$  satisfies the Sommerfeld radiation condition, which requires that

$$\frac{\partial p}{\partial r} - ikp = \mathcal{O}(1/r), \quad r \rightarrow \infty. \tag{11}$$

### 3 Boundary integral formulas for the acoustic pressure

In the previous section it has been shown that the acoustic pressure in the closed domain  $\Omega_1$  (partly filled with porous material and partly with air) and in the half-space  $\Omega_i$  above the trim panel is governed by the Helmholtz equation (for air (1) and for the porous medium (2)). In this section boundary integral formulas for the acoustic pressure are presented which satisfy the Helmholtz equation. First, a formula is given for the acoustic pressure in the half-space  $\Omega_i$  and second a symmetric formula is derived for a closed domain  $\Omega$  (in terms of the previous section  $\Omega$  is defined either by the domain  $\Omega_{1,a}$  or by the domain  $\Omega_{1,g}$ ). In the following sections the Green-function  $G$  for the Helmholtz equation in an infinite domain is used,

$$G_\alpha(r, r') = \frac{e^{i\alpha|r-r'|}}{4\pi|r-r'|}, \quad r \neq r', \quad (12)$$

with  $\alpha = k$  for waves propagating in air and with  $\alpha = \gamma$  (as defined in (3)) for waves propagating in the porous medium.

#### 3.1 Boundary integral formula for the half-space $\Omega_i$

The vibrating trim panel is baffled in a perfectly rigid plane given by  $\Gamma_\infty$ . The boundary integral formula for the acoustic pressure in the half-space  $\Omega_i$  is given by the single layer potential ansatz

$$\begin{aligned} p(r) &= (V_k\phi)(r), \quad r \in \Omega_i, \\ V_k\phi(r) &= \int_{\Gamma_3} G_k(r, r')\phi(r') d\Gamma(r'), \quad r \in \Omega_i. \end{aligned} \quad (13)$$

with the single layer given by

$$\phi(r) = -2\rho_a\omega^2 w(r), \quad r \in \Gamma_3. \quad (14)$$

It can be shown that this single layer potential satisfies the Helmholtz equation and the boundary conditions (5), (6) and (11). This follows from classical results of potential theory. The integral operator  $V_k$  is weakly singular, so that (13) is also well defined for  $r \in \Gamma_3$ , i.e.

$$p(r) = (V_k\phi)(r), \quad r \in \Gamma_3. \quad (15)$$

Note that  $V_k$  is a symmetric operator, because  $G_k$  is symmetric with respect to  $r$  and  $r'$ .

### 3.2 Boundary integral formula for a closed domain $\Omega$

Let  $\Omega \subset \mathbb{R}^3$  be a bounded domain with piecewise smooth boundary  $\partial\Omega$ . In terms of the previous section  $\Omega$  is defined either by the sub-domain  $\Omega_{1,a}$  or by the sub-domain  $\Omega_{1,g}$ . Note that the boundary of  $\Omega_{1,a}$  is given by  $\partial\Omega_{1,a} = \Gamma_{2,a} \cup \Gamma_3 \cup S$ , while the boundary of  $\Omega_{1,g}$  is given by  $\partial\Omega_{1,g} = \Gamma_{2,g} \cup \Gamma_1 \cup S$  ( $\Gamma_{2,a}$  and  $\Gamma_{2,g}$  are the parts adjoining the air and the porous medium, respectively).

For the acoustic pressure the following representation formula holds

$$p(r) = \int_{\partial\Omega} G_\alpha(r, r') \partial_{n'} p(r') d\Gamma(r') - \int_{\partial\Omega} \partial_{n'} G_\alpha(r, r') p(r') d\Gamma(r'). \quad (16)$$

Define the following boundary integral operators

$$\begin{aligned} V_\alpha \phi(r) &:= \int_{\partial\Omega} G_\alpha(r, r') \phi(r') d\Gamma(r'), & r \in \partial\Omega, \\ K_\alpha \phi(r) &:= \int_{\partial\Omega} \partial_{n'} G_\alpha(r, r') \phi(r') d\Gamma(r') & r \in \partial\Omega, \\ K'_\alpha \phi(r) &:= \partial_n \int_{\partial\Omega} G_\alpha(r, r') \phi(r') d\Gamma(r') & r \in \partial\Omega, \\ D_\alpha \phi(r) &:= -\partial_n \int_{\partial\Omega} \partial_{n'} G_\alpha(r, r') \phi(r') d\Gamma(r'), & r \in \partial\Omega. \end{aligned}$$

The representation formula (16) and the jump relations for single and double layer potentials lead to the following boundary integral equations on  $\partial\Omega$

$$p = V_\alpha \partial p - K_\alpha p + \frac{1}{2} p = V_\alpha \partial p + \left(\frac{1}{2} I - K_\alpha\right) p \quad (17)$$

$$\partial p = D_\alpha p + K'_\alpha \partial p + \frac{1}{2} \partial p \quad (18)$$

In most boundary element calculations in acoustics the first equation (17) is being used for sound predictions. For some applications also the second one is used. However, the discretization of these boundary integral equations result in general in non-symmetric system matrices, which have fictitious eigenvalues and eigenvectors. The equations (17) and (18) can be rewritten as

$$p = \left(\frac{1}{2} I + K_\alpha\right)^{-1} V_\alpha \partial p \quad (19)$$

$$p = D_\alpha^{-1} \left( \frac{1}{2} I - K'_\alpha \right) \partial p \quad (20)$$

Observe that the operators  $(\frac{1}{2} I + K_\alpha)^{-1} V_\alpha$  and  $D_\alpha^{-1} (\frac{1}{2} I - K'_\alpha)$  define so called Poincaré-Steklov operators mapping

$$\partial p \rightarrow p |_{\partial\Omega} .$$

The operators in (19) and (20) are not symmetric, while the weak formulation of (1): find  $p \in H^1(\Omega)$  such that

$$\int_{\Omega} (\nabla p \cdot \nabla \psi - \alpha^2 p \psi) dA - \int_{\partial\Omega} \frac{\partial p}{\partial n} \psi dS = 0, \quad (21)$$

for all test functions  $\psi \in H^1(\Omega)$ , yields (with restriction of  $p$  to  $\partial\Omega$ ) a symmetric Poincaré-Steklov operator. The boundary element discretization of (17) or (18) will result in a non-symmetric boundary element matrix. Therefore, the boundary element discretization of (17) or (18) will not have the same mapping properties as the finite element discretization of (21). It has been shown in Ref. 1 that a symmetric boundary element discretization of a Poincaré-Steklov operator can be obtained by substituting (20) into (17). The result becomes

$$p = T_\alpha \partial p \quad (22)$$

with

$$T_\alpha = V_\alpha + \left( \frac{1}{2} I - K_\alpha \right) D_\alpha^{-1} \left( \frac{1}{2} I - K'_\alpha \right). \quad (23)$$

Note that  $T_\alpha$  defines a symmetric Poincaré-Steklov operator, since  $V_\alpha$  and  $D_\alpha$  are symmetric. The discretization of  $T_\alpha$  involves, however, the approximation of the hypersingular operator  $D_\alpha$ , the weakly singular operator  $V_\alpha$  and the regular operator  $K_\alpha$ . The hypersingular operator can be regularized by integration of parts and the integrals reduce to weakly singular integrals. The coefficients of the boundary element matrices of the operators  $D_\alpha$  and  $V_\alpha$  can be evaluated simultaneously so that the computational costs are comparable with the costs of the discretization of (17) or (18).

## 4 Boundary element discretization

The integral operators  $V_k$  of (15) and  $T_\alpha$  of (23) are discretized using a Galerkin boundary element method. The trial spaces are given by the piecewise linear basis functions  $\{w_l\}_{l=1}^N$  on a triangular surface mesh with  $N$  nodes and  $M$  elements  $\{S_k\}_{k=1}^M$ . Following ref. 1 one obtains the following boundary element discretization for the operator  $T_\alpha$

$$T_{\alpha,h} = M_h^{-1} \mathcal{V}_{\alpha,h} M_h^{-1} + \left(\frac{1}{2}I_h - M_h^{-1} \mathcal{K}_{\alpha,h}\right) D_{\alpha,h}^{-1} \left(\frac{1}{2}I_h - \mathcal{K}'_{\alpha,h} M_h^{-1}\right), \quad (24)$$

with

$$\begin{aligned} (M_h)_{l,j} &= (w_l, w_j), \\ (\mathcal{V}_{\alpha,h})_{l,j} &= (V_\alpha w_l, w_j), \\ (\mathcal{K}_{\alpha,h})_{l,j} &= (K_\alpha w_l, w_j), \\ (\mathcal{K}'_{\alpha,h})_{l,j} &= (\mathcal{K}_{\alpha,h})_{j,l} \\ (D_{\alpha,h})_{l,j} &= (D_\alpha w_l, w_j). \end{aligned}$$

Note that (24) defines a symmetric boundary element matrix, because  $\mathcal{V}_{\alpha,h}$  and  $D_{\alpha,h}$  are symmetric.

The calculation of the matrix element  $(D_{\alpha,h})_{l,j}$  involves the evaluation of a hypersingular integral, since

$$(D_\alpha w_l, w_j) = - \int_\Gamma \int_\Gamma \frac{\partial^2 G_\alpha}{\partial n \partial n'}(r, r') w_l(r) w_j(r') d\Gamma(r) d\Gamma(r'),$$

where the second integral must be interpreted as a finite part integral for  $r \in \Gamma$ . The hypersingular integral can be regularized by integration of parts using the fact that  $G_\alpha$  is the fundamental solution of the Helmholtz operator (See e.g. ref. 3). It can be shown that

$$\begin{aligned} (D_\alpha w_l, w_j) &= \int_\Gamma \int_\Gamma G_\alpha(r, r') \langle n_r \times \nabla_r w_l(r), n_{r'} \times \nabla_{r'} w_j(r') \rangle d\Gamma(r) d\Gamma(r') \\ &\quad - \alpha^2 \int_\Gamma \int_\Gamma w_l(r) w_j(r') G_\alpha(r, r') \langle n_r, n_{r'} \rangle d\Gamma(r) d\Gamma(r') \end{aligned} \quad (25)$$

Observe that (25) only contains weakly singular integrals.

## 5 Numerical implementation

Let the nodes of the finite element mesh be given by  $\{r_l\}_{l=1}^N$ . On each triangular element  $S_k$  three local linear functions  $\psi_i^k(r)$ ,  $i = 1, 2, 3$  are introduced, which yield the value 1 at the  $i$ -th vertex of  $S_k$  and 0 at the other two vertices of  $S_k$ . Indirect addresses are used to associate vertices of a triangular element with the node numbers of the mesh, i.e. there exists an array  $nn(i, k)$  yielding the node number of the  $i$ -th vertex of the  $k$ -th triangular element. The basis and test functions are continuous functions of the form

$$\mu(r) = \sum_{k=1}^M \sum_{i=1}^3 \mu_i^k \psi_i^k(r),$$

where  $\mu_i^k$  is the value of the function  $\mu$  at the node  $r_l$  with  $l = nn(i, k)$ .

With this set of basis and test functions the form  $(D_\alpha \xi, \mu)$  can be rewritten as

$$(D_\alpha \xi, \mu) = \sum_{l=1}^M \sum_{j=1}^3 \sum_{k=1}^M \sum_{i=1}^3 D_{j,i}^{l,k} \xi_j^l \mu_i^k \quad (26)$$

where

$$\begin{aligned} D_{j,i}^{l,k} &= \int_{S_l} \int_{S_k} \alpha^2 \langle n_{S_l}, n_{S_k} \rangle \psi_i^k(r') \psi_j^l(r) G_\alpha(r, r') d\Gamma(r') d\Gamma(r), \\ &- \int_{S_l} \int_{S_k} \langle n_{S_l} \times \nabla \psi_j^l, n_{S_k} \times \nabla \psi_i^k \rangle G_\alpha(r, r') d\Gamma(r') d\Gamma(r). \end{aligned} \quad (27)$$

The matrix elements  $\mathcal{V}_{j,i}^{l,k}$ ,  $\mathcal{K}_{j,i}^{l,k}$  and  $M_{j,i}^{l,l}$ , which follow from substituting the basis and test functions into  $(V_\alpha \xi, \mu)$ ,  $(K_\alpha \xi, \mu)$  and the mass-matrix  $(\xi, \mu)$ , can be obtained in a similar way,

$$\mathcal{V}_{j,i}^{l,k} = \int_{S_l} \int_{S_k} \psi_i^k(r') \psi_j^l(r) G_\alpha(r, r') d\Gamma(r') d\Gamma(r), \quad (28)$$

$$\mathcal{K}_{j,i}^{l,k} = \int_{S_l} \int_{S_k} \frac{-1 + i\alpha|r - r'|}{4\pi} \frac{e^{i\alpha|r - r'|}}{|r - r'|^2} \langle n(r'), \frac{r' - r}{|r' - r|} \rangle \psi_i^k(r') \psi_j^l(r) d\Gamma(r') d\Gamma(r), \quad (29)$$

$$M_{j,i}^{l,l} = \int_{S_l} \psi_j^l(r) \psi_i^l(r) d\Gamma(r). \quad (30)$$

The coefficients of the global boundary element matrices of the previous section (related to the unknown quantities at the nodes) are obtained by assembling the local boundary element matrices,

e.g. the coefficients  $(\mathcal{V}_{\alpha,h})_{p,q}$  follow from summing the influence coefficients  $V_{j,i}^{l,k}$  for which  $nn(j,l) = p$  and  $nn(i,k) = q$ , i.e.

$$(\mathcal{V}_{\alpha,h})_{p,q} = \sum_{l=1}^M \sum_{\substack{j=1 \\ nn(j,l)=p}}^3 \sum_{k=1}^M \sum_{\substack{i=1 \\ nn(i,k)=q}}^3 V_{j,i}^{l,k}.$$

Analogously  $(D_{\alpha,h})_{p,q}$ ,  $(\mathcal{K}_{\alpha,h})_{p,q}$  and  $(M_h)_{p,q}$  are obtained. The matrix  $\mathcal{K}'_{\alpha,h}$  can be obtained from transposing the matrix  $\mathcal{K}_{\alpha,h}$ .

Note that the derivatives of  $\psi_j^l(r)$  are constant for  $r \in S_l$ , since the basis functions are piecewise linear. As a consequence the terms between brackets  $\langle \rangle$  in (27) are constant. Therefore, the evaluation of the influence coefficients  $D_{j,i}^{l,k}$  in (27),  $\mathcal{V}_{j,i}^{l,k}$  in (28) and  $\mathcal{K}_{j,i}^{l,k}$  in (29) requires only the calculation of the following boundary integrals

$$\int_{S_l} \int_{S_k} \psi_i^k(r') \psi_j^l(r) G_{\alpha}(r, r') d\Gamma(r') d\Gamma(r), \quad (31)$$

$$\int_{S_l} \int_{S_k} G_{\alpha}(r, r') d\Gamma(r') d\Gamma(r), \quad (32)$$

and

$$\int_{S_l} \int_{S_k} \frac{-1 + i\alpha|r - r'|}{4\pi} \frac{e^{i\alpha|r-r'|}}{|r - r'|^2} \langle n(r'), \frac{r' - r}{|r' - r|} \rangle \psi_i^k(r') \psi_j^l(r) d\Gamma(r') d\Gamma(r). \quad (33)$$

The calculation of the singular integrals in (27) and (28) has been described in Ref. 4. They are approximated by use of a Gauss quadrature rule for the outer integral and a regularizing coordinate transformation for the inner integral. This approach is also used for the evaluation of the nearly singular integrals in (27) and (28), i.e. the regular integrals for which the distance of  $S_k$  to  $S_l$  is small.

It remains to calculate  $\mathcal{K}_{j,i}^{l,k}$  for  $k \neq l$ . Note that  $\mathcal{K}_{j,i}^{k,k} = 0$  for flat elements since  $\langle n(r'), \frac{r' - r}{|r' - r|} \rangle = 0$  for  $r, r' \in S_k$ . The coefficients  $\mathcal{K}_{j,i}^{l,k}$  are computed by applying a Gauss quadrature rule, i.e.  $\mathcal{K}_{j,i}^{l,k}$  is approximated by

$$\frac{4|S_l||S_k|}{4\pi} \sum_{n=1}^{N_G} \sum_{m=1}^{N_G} w_n w_m (-1 + i\alpha|r_n - r'_m|) \frac{e^{i\alpha|r_n - r'_m|}}{|r_n - r'_m|^2} \langle n_{S_k}, \frac{r'_m - r_n}{|r'_m - r_n|} \rangle \psi_i^k(r'_m) \psi_j^l(r_n), \quad (34)$$

where  $|S_k|$  is the area of the triangular element  $S_k$ ,  $n_{S_k}$  the unit normal on  $S_k$  and  $N_G$  the number of Gauss points. The weights of the Gauss quadrature rule sum up to  $\frac{1}{2}$ .

The integral  $M_{j,i}^{l,l}$  is easily calculated. For  $i = j$  the exact value is  $|S_i|/18$  and for  $i \neq j$  the exact value is  $|S_i|/24$ .

## 6 Numerical results

The symmetrical boundary element formulation has been implemented in the modular finite element program B2000 and has been coupled with the existing finite element code for the structural analysis of plates and shells. The boundary element formulation is applied to the acoustic-structural analysis of a double panel configuration. The structure consists of two identical aluminium plates with a length of 1.46 m and a width of 0.76 m (see figure 2), which are clamped at all edges. The distance between the plates is 0.1 m. The gap between the plates is either filled by air or by glass-wool. The eigenfrequencies of this double panel configuration and its environment are computed. The results are compared with a finite element code where the acoustic pressure was obtained by the numerical solution of (21) using 20-noded acoustic elements.

The elastomechanics of the plates is modelled by putting 100 linear quadrilateral finite shell elements on each plate. The basic properties of the aluminium plates are: modulus of elasticity =  $7.0E+10$  N/m<sup>2</sup>, Poisson's ratio = 0.3, density = 2800 kg/m<sup>3</sup> and thickness = 0.0025 m.

In the first example the cavity between the plates is filled with air. The air surrounding the plates can also be modelled, but is left out here, to be able to compare the results with the finite element acoustic calculations. The properties of air are:  $\rho_a = 1.2$  kg/m<sup>3</sup> and  $c = 340$  m/s.

The boundary element surface discretization consists of 200 triangular elements on each plate (in such a way that the nodes correspond with the nodes of the structural quadrilateral elements) and 320 triangular elements on the four vertical faces to close the cavity between the plates. The first five eigenfrequencies computed are given in the second column of table 1. In the third column of table 1 the results are shown of the finite element acoustic calculations. A good agreement of the results is observed between both methods. The small differences are due to differences in the numerical methods, e.g. integration rules.

In the second example the cavity between the plates is filled with glass-wool, having the following properties:  $\rho_e = 1.2$  kg/m<sup>3</sup>,  $c_e = 290$  m/s,  $M = 2267$  kg/m<sup>3</sup>,  $h = 0.9955$  and  $\sigma = 2.3E4$  Ns/m<sup>3</sup>. Note that the complex wavenumber (as defined in (3)) depends on the frequency  $\omega$ , so that the coupled eigenvalue problem becomes non-linear. The same number of elements has been used as in the first example. The first five eigenfrequencies as computed by the symmetrical boundary element approach and the acoustic finite limp element model are given in the fourth and fifth column of table 1. The eigenfrequencies are complex valued due to energy dissipation. Again small differences are observed between the two numerical methods. For this example the

differences are also due to the non-linearity of the eigenvalue problem. In order to solve the eigenvalue problem an initial value of  $\omega$  has to be specified to calculate  $\kappa(\omega)$  in (3). The results of table 1 have been obtained taking a value close to the real part of the eigenfrequency. When, however, a value of 30 Hz ( $\omega = 60\pi$  rad /s) would have been chosen for the calculation of  $\kappa(\omega)$ , the first eigenfrequency would have been  $7.84+i*0.190$ , showing the dependency of the problem on the initial value of  $\kappa(\omega)$ .

medium:	air		glass-wool	
MODE	BEM	FEM	BEM	FEM
1	11.95	12.27	$7.46+i*0.161$	$7.84+i*0.081$
2	13.16	13.16	$12.73+i*0.019$	$12.62+i*0.018$
3	20.83	21.02	$14.97+i*0.188$	$15.05+i*0.153$
4	21.93	21.93	$21.21+i*0.054$	$21.93+i*0.049$
5	36.98	37.14	$29.61+i*0.657$	$29.29+i*0.466$

Table 1 Eigenfrequencies [Hz] of double panel configuration

## 7 Conclusions

A symmetrical boundary element formulation has been described for the sound transmission through a cabin wall of an aircraft. The computational costs of the presented boundary element formulation are comparable with the costs of classical boundary element formulations in acoustics. This could be achieved by regularizing the hypersingular integral operator and by computing the coefficients of the boundary element matrices of the weakly singular and hypersingular integral operators simultaneously.

The symmetrical boundary element formulation has been applied to compute the eigenfrequencies of the coupled acoustic-structural problem of a double panel configuration where the cavity between the panels was filled by either air or by glass-wool. The computed eigenfrequencies of this coupled problem show a fair agreement with results of a code where both the elastomechanics of the panels and the acoustic pressure was modelled by finite elements. In a forthcoming paper the described boundary element formulation will be applied to a double panel configuration where the cavity is partly filled by air and partly by glass-wool.

## 8 References

1. SCHMIDT, G.; Boundary element discretization of Poincaré-Steklov operators, *Numer. Math.*, Vol. 69, 1994, pp. 83-101.
2. GORANSSON, P.; Acoustic Finite Element Formulation of a Flexible Porous Material - A Correction for Inertial Effects, *Journal of Sound and Vibration*, Vol. 185, 1995, pp. 559-580.
3. MAUE, A.W.; Toward formulation of a general diffraction problem via an integral equation, *Zeitschrift für Physik*, Vol. 126, 1949, pp. 601-618.
4. KOELINK, H.T., SCHIPPERS, H., HEIJSTEK, J.J., DERKSEN, J.J.; Modal analysis of solar arrays using boundary integral equations, NLR TP 92281 L (1992), in *Boundary Elements XIV, Vol 2: Stress Analysis and Computational Aspects*, C.A. Brebbia, J. Dominguez, F. Paris, eds., Computational Mechanics Publ. & Elsevier Science Publ., 1992, pp. 515-525.

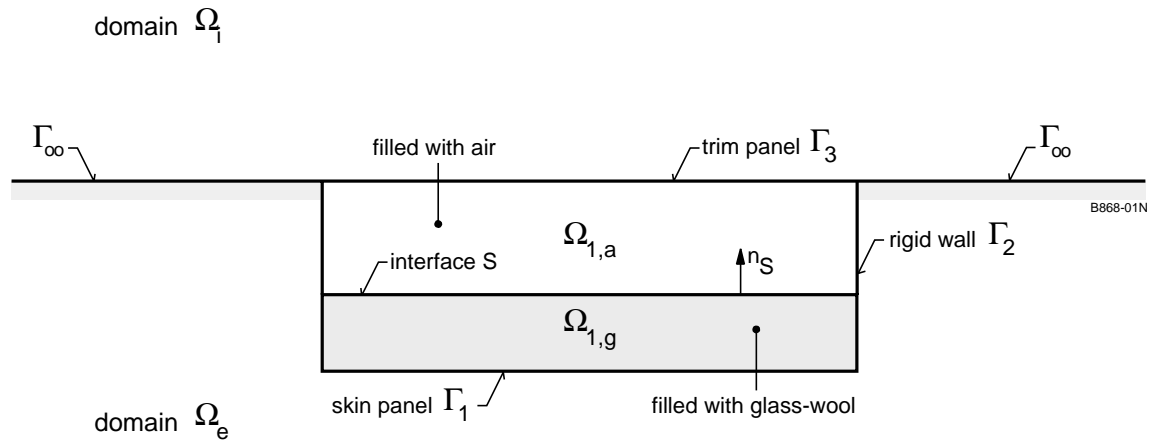


Fig. 1 Cross section of baffled double wall configuration

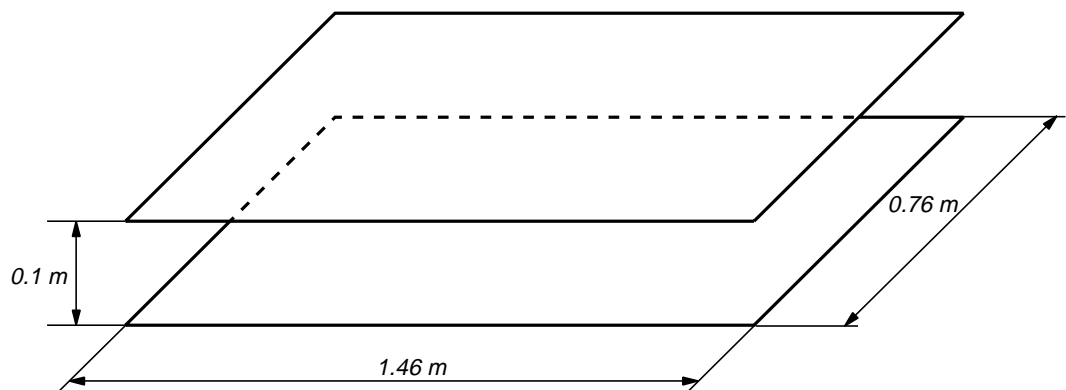


Fig. 2 Two panels clamped at the edges at a distance from each other